UiO : University of Oslo

INF5410 Array signal processing.
Ch. 3: Apertures and Arrays

Endrias G. Asgedom

Department of Informatics, University of Oslo

February 2012

Outline

Finite Continuous Apetrures
- Apertures and Arrays
- Aperture function
- Classical resolution
- Geometrical optics
- Ambiguities & Aberrations

Spatial sampling
- Sampling in one dimension

Arrays of discrete sensors
- Regular arrays
- Grating lobes
- Element response
- Irregular arrays

Outline

Apertures and Arrays

- *Aperture*: a spatial region that transmits or receives propagating waves.
- *Array*: Group of sensors combined in a discrete space domain to produce a single output.
- To observe a wavefield at *m*'th sensor position, $\vec{x}_m$, we distingush:
  - Fields value: $f(\vec{x}_m, t)$.
  - Sensors output: $y_m(t)$.

  e.g If sensor is *perfect* (i.e. linear transf., infinite bandwidth, omni-directional):

$$y_m(t) = \kappa \cdot f(\vec{x}_m, t), \ \kappa \in \Re \text{ (or } \mathcal{C}).$$

Aperture function

- Our sensors gather a space-time wavefield only over a finite area.
- Omni-directional sensors: have no directional preference. E.g Sensors in a seismic exploration study.
- Directional sensors: have significant spatial extent.
  - They spatially integrate energy over the aperture, i.e. they focus in a particular propagation direction. E.g Parabolic dish.
  - They are described by the aperture function, $w(\vec{x})$, which describes:
    - Spatial extent reflects size and shape
    - Aperture weighting: relative weighting of the field within the aperture (also known as shading, tapering, apodization).

Aperture smoothing function ($\neq$ Sec. 3.1.1)

- Aperture function at $\vec{\xi}$: $w(\vec{\xi})$
- Field recorded at $\vec{\xi}$: $f(\vec{x} - \vec{\xi}, t)$
- contribution from the area $\delta\vec{\xi}$ at $\vec{\xi}$ for a monochromatic wave with angular frequency ω is: $w(\vec{\xi})f(\vec{x} - \vec{\xi}, \omega)d\vec{\xi}$
- contribution of the full sensor
  $z(\vec{x}, \omega) = \int_{aperture} w(\vec{\xi})f(\vec{x} - \vec{\xi}, \omega)d\xi.$
  $z(\vec{x}, \omega) = w(\vec{x}) * f(\vec{x}, \omega).$
  $Z(\vec{k}, \omega) = W(\vec{k})F(\vec{k}, \omega).$

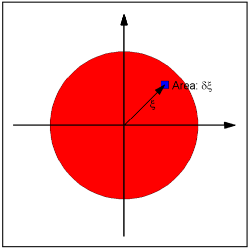

Aperture smoothing function ...

- Aperture smoothing function:
  $W(\vec{k}) = \int_{-\infty}^{\infty} w(\vec{x}) \exp(j\vec{k}.\vec{x}) d\vec{x}$
- The wavenumber-frequency spectrum of the field:
  $F(\vec{k}, \omega) = \int_{-\infty}^{\infty} \int_{-\infty}^{\infty} f(\vec{x}, t) \exp(j\vec{k}.\vec{x} - \omega t) d\vec{x} dt$
- Assume a single plane wave, propagating in direction
  $\vec{\zeta}^0, \vec{\zeta}^0 = \vec{k}^0 / k$
  $\Rightarrow \; f(\vec{x}, t) = s(t - \vec{\alpha}^0 \cdot \vec{x}), \; \vec{\alpha}^0 = \vec{\zeta}^0 / c$
  $\Rightarrow \; F(\vec{k}, \omega) = S(\omega)\delta(\vec{k} - \omega\vec{\alpha}^0)$ (Sec. 2.5.1)

This prop. wave contains energy only along the line $\vec{k} = \omega\vec{\alpha}^0$ in wavenumber-frequency space.

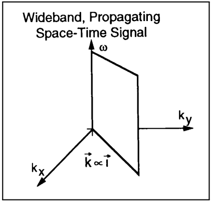

Aperture smoothing function ...

- Subst. of $F(\vec{k},\omega) = S(\omega)\delta(\vec{k} - \omega\vec{\alpha}^0)$ into $Z(\vec{k},\omega) = W(\vec{k})F(\vec{k},\omega)$ gives

$$Z(\vec{k},\omega) = W(\vec{k})S(\omega)\delta(\vec{k} - \omega\vec{\alpha}^0)$$

$$Z(\vec{k},\omega) = W(\vec{k} - \omega\vec{\alpha}^0)S(\omega)$$

- For $\vec{k} = \omega\vec{\alpha}^0 \Rightarrow Z(\omega\vec{\alpha}^0,\omega) = W(0)S(\omega)$: The information from the signal $s(t)$ is preserved.
- For $\vec{k} \neq \omega\vec{\alpha}^0$: The information from the signal $s(t)$ gets filtered.

Aperture smoothing function ...

- Linear aperture:

  $b(x) = 1, \ |x| \leq D/2$

  $\Rightarrow W(\vec{k}) = \frac{\sin k_x D/2}{k_x/2}$

  $\Rightarrow$ Sidelobe at $k_{x_0} \approx 2.86\pi/D$

  $|W(k_{x_0}| \approx 0.2172D \ \Rightarrow$

  $\frac{\text{ML}}{\text{SL}} \approx \frac{D}{0.2172} = 4.603 \propto$ 13.3dB

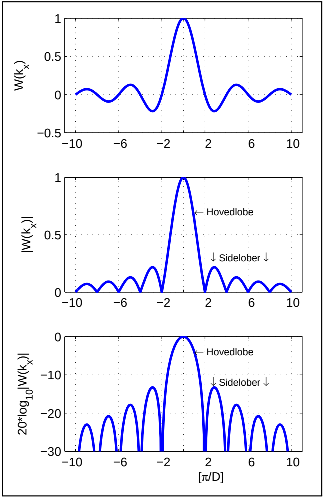

Aperture smoothing function ...

- Circular aperture:
  $o(x, y) = 1, \sqrt{x^2 + y^2} \leq R$
  $\Rightarrow O(k_{xy}) = \frac{2\pi R}{k_{xy}} J_1(k_{xy} R)$
- $\Rightarrow$ SL at $k_{xy_0} \approx 5.14/R$
  $\frac{\text{ML}}{\text{SL}} \approx 7.56 \propto -17.57\text{dB}$.

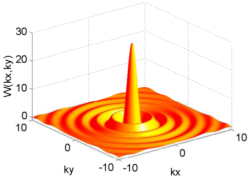

Classical resolution

- Spatial extent of $w(\vec{x})$ determines the resolution with which two plane waves can be separated.
- Ideally, $W(\vec{k}) = \delta(\vec{k})$, i.e. infinite spatial extent!

Rayleigh criterion: *Two incoherent plane waves, propagating in two slightly different directions, are resolved if the mainlobe peak of one aperture smoothing function replica falls on the first zero of the other aperture smoothing function replica, i.e. half the mainlobe width.*

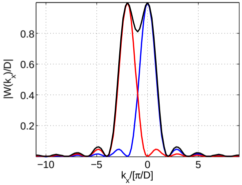

Classical resolution ...

- Linear aperture of size D

$$W(k_x) = \frac{\sin(k_x D/2)}{k_x/2} (= D\text{sinc}(k_x D/2)) = \frac{\sin(\pi \sin\theta D/\lambda)}{\pi \sin\theta/\lambda}$$

  - -3 dB width: $\theta_{-3dB} \approx 0.89\lambda/D$
  - -6 dB width: $\theta_{-6dB} \approx 1.21\lambda/D$
  - Zero-to-zero distance: $\theta_{0-0} = 2\lambda/D$

- Circular aperture of diameter D

$$W(k_{xy}) = \frac{2\pi D/2}{k_{xy}} J_1(k_{xy} D/2)$$

  - -3 dB width: $\theta_{-3dB} \approx 1.02\lambda/D$
  - -6 dB width: $\theta_{-6dB} \approx 1.41\lambda/D$
  - Zero-to-zero distance: $\theta_{0-0} \approx 2.44\lambda/D$

- Rule-of-thumb; Angular resolution: $\theta = \lambda/D$

Geometrical optics

- Validity: down to about a wavelength
- Near field-far field transition
  - $d_R = D^2/\lambda$ for a maximum phase error of $\lambda/8$ over aperture
- f-number
  - Ratio of range and aperture: $f_\# = R/D$
- Resolution
  - Angular resolution: $\theta = \lambda/D$
  - Azimuth resolution: $u = R\theta = f_\#\lambda$
- Depth of focus
  - Aperture is focused at range R. Phase error of $\lambda/8$ yields $r = \pm f_\#^2\lambda$ or DOF=$2f_\#^2\lambda$ (proportional to phase error)

Geom.Opt: Near field/Far field crossover

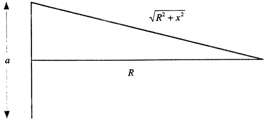

(2.1)

The differential path length Δ associated with a point x on the aperture and a range R can be evaluated using simple geometry.

$$\begin{aligned}\Delta &= \sqrt{R^2 + x^2} - R \\ &= R\sqrt{1 + \left(\frac{x}{R}\right)^2} - R \\ &\cong \frac{x^2}{2R}\end{aligned} \tag{2.2}$$

This differential error across the aperture is thus essentially quadratic, and can be reduced arbitrarily be increasing R. That is, in the far field the radiation from each point on the aperture arrives (essentially) coherently, adding constructively. As we move the point target closer to the aperture, the delay error increases inversely with R until, at some crossover range R_C between the near field and far field, it becomes non-negligible. We define this range $R = R_C$ (rather arbitrarily) as that for which the maximum error is

$$\Delta = \lambda/8 \tag{2.3}$$

As the maximum error will always be associated with the ends of the aperture, we substitute $x = a/2$ and use $\Delta = \lambda/8$ in eq. (2.2) to obtain

$$\boxed{\frac{R_C}{a} = \frac{a}{\lambda}} \tag{2.4}$$

That is, *the crossover range, measured in apertures, is equal to the aperture, measured in wavelengths.*

The far field is often called the *Fraunhofer region*, where we can ignore the differential phase terms associated with different propagation lengths. The near field is often called the *Fresnel region*, characterized by the (approximately) quadratic phase attributable to different propagation lengths from different aperture points.

Let us calculate the near field/far field crossover of a practical ultrasonic aperture operating at a center frequency of 3.5 MHz. Let

$$a = 28mm$$
$$\lambda = .44mm$$

This aperture might have 128 elements spaced at $\lambda/2$. The transition between the Fraunhofer region and the Fresnel region occurs at

$$R_C = 1782mm$$

or almost two meters! *All modern diagnostic ultrasonic imaging occurs in the extreme near field.* This distinguishes the discipline from many other imaging technologies and presents a notable engineering challenge.

(From Wright: *Image Formation ...*)

Geom.Opt: Near field/Far field crossover

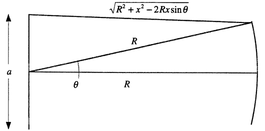

(2.5)

The differential path length Δ between an aperture point x and the center, as our point target moves along the circular arc, is

$$\begin{aligned}\Delta &= \sqrt{R^2 + x^2 - 2Rx\sin\theta} - R \\ &= R\sqrt{1 + \left(\frac{x}{R}\right)^2 - 2\left(\frac{x}{R}\right)\sin\theta} - R\end{aligned} \quad (2.6)$$

Expanding this in terms of x/R and θ $\quad \sqrt{1+b} \approx 1 + \frac{b}{2}$, $b \ll 1$; $\sin\theta \approx \theta$, $\theta \ll 1$

$$\begin{aligned}\Delta &\cong -x\theta + \frac{x^2}{2R} \\ &\cong -x\theta\end{aligned} \quad (2.7)$$

As in the last section, we ignore the quadratic term on the basis of far field operation.

Destructive interference occurs when the magnitude of any differential path length error exceeds $\lambda/4$, so we want to calculate the angular extent for which

$$-\lambda/4 \le \Delta \le \lambda/4 \quad (2.8)$$

As the maximum error will always be associated with the ends of the aperture, we substitute $x = \pm a/2$ and use $\Delta = \pm\lambda/4$ in eq. (2.7) to get the angles associated with this maximum error.

$$\theta\big|_{\Delta=\pm\lambda/4} = \pm\frac{\lambda}{2a} \quad (2.9)$$

We define this angular extent as the angular resolution θ_R.

$$\boxed{\theta_R = \frac{\lambda}{a}} \quad (2.10)$$

That is, *the angular resolution, measured in radians, is the inverse of the aperture, measured in wavelengths.*

It is also convenient to define the ratio of the range and the aperture, which re-occurs in different contexts, as the f-number.

$$\boxed{f_\# = \frac{R}{a}} \quad (2.11)$$

The distance around the circular arc associated with θ_R is simply $R\theta_R$, yielding the azimuthal resolution u_R.

$$\boxed{u_R = f_\#\lambda} \quad (2.12)$$

That is, *the azimuthal resolution, measured in wavelengths, is the f-number.*

(From Wright: *Image Formation ...*)

Geom.Opt: Near field/Far field crossover

<u>Depth of Focus of a Focused Linear Aperture</u>

We can bring the far field diffraction pattern into the near field by *focusing* the aperture. This is done by applying compensating delays to incremental portions of the aperture. (In the figure below, we show the compensating delays as corrections to path length.)

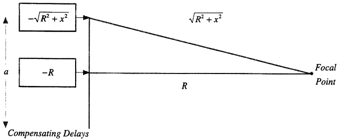

(2.15)

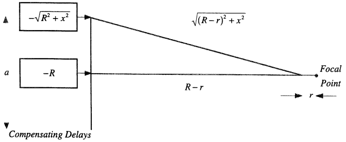

(2.16)

The differential delay between the center of the aperture and any other aperture point x (including the compensating delays) is

$$\begin{aligned}\Delta &= \left[\sqrt{(R-r)^2+x^2}-\sqrt{R^2+x^2}\right]-\left[(R-r)-R\right]\\ &= R\left[\sqrt{\left(1-\frac{r}{R}\right)^2+\left(\frac{x}{R}\right)^2}-\sqrt{1+\left(\frac{x}{R}\right)^2}+\left(\frac{r}{R}\right)\right]\end{aligned} \tag{2.17}$$

Expanding this in a two dimensional Taylor's series in terms of r/R and x/R and keeping the lowest order term yields

$$\Delta = \frac{x^2 r}{2R^2} \tag{2.18}$$

The delay error across the aperture is thus seen to be essentially linear in r and quadratic in x. As we move closer to the aperture, the sign of the error is positive, and further away yields a negative error. Similar to our analysis of the near field/far field crossover, we define the depth of focus as the extent of the incremental range r for which

$$-\lambda/8 \le \Delta \le \lambda/8 \tag{2.19}$$

over the aperture. Substituting $x = a/2$ and $\Delta = \pm\lambda/8$ into eq. (2.18), and using $f_{\#} = R/a$, we see that the depth of focus is bounded by

$$r\big|_{\Delta=\pm\lambda/8} = \pm f_{\#}^2\lambda \tag{2.20}$$

so the total depth of focus r_D is

$$\boxed{r_D = \pm f_{\#}^2\lambda = 2f_{\#}^2\lambda} \tag{2.21}$$

That is, *the one-sided depth of focus, measured in wavelengths, is the square of the f-number.* Other definitions for r_D can be found in the literature, based on criteria other than the $\lambda/8$ differential error we have employed here. Let us look at the effects of moving our point target to the edge of the depth of focus and beyond.

(From Wright: *Image Formation ...*)

Ultrasound imaging

- Near field/far field transition, D=28mm, f=3.5MHz $\Rightarrow$
  - $\lambda = 1540/3.5 \cdot 10^6 = 0.44$mm and $d_R = D^2/R = 1782$mm
  - All diagnostic ultrasound imaging occurs in the extreme near field!
- Azimuth resolution, D=28mm, f=7MHz $\Rightarrow$
  - $\lambda = 0.22$mm and $\theta = \lambda/D = 0.45^\circ$,
  - i.e. about 200 lines are required to scan $\pm 45^\circ$
- Depth of focus, $f_\# = 2$, f=5MHz $\Rightarrow$
  - $\lambda = 0.308$mm and DOF = $2f_\#^2\lambda \approx 2.5$mm.
  - Ultrasound requires $T = 2 \cdot 2.5 \cdot 10^{-3}/1540 = 3.2\mu$s to travel the DOF. This is the minimum update rate for the delays in a dynamically focused system.

Ambiguities & Aberrations

- Aperture ambiguities
  - Due to symmetries
- Aberrations
  - Deviation in the waveform from its intended form.
  - In optics; due to deviation of a lens from its ideal shape.
  - More generally; Turbulence in the medium, inhomogeneous medium or position errors in the aperture.
  - Ok if small comp. to λ_0.

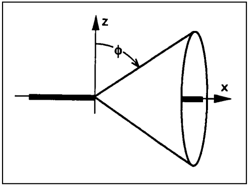

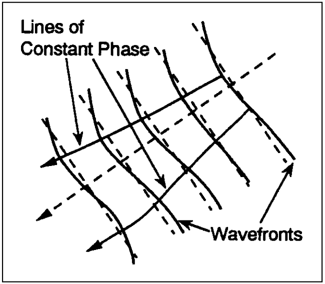

$\phi \longleftrightarrow$ 'sin ϕ'

- $\vec{k}$ represents two kind of information
  1. $|\vec{k}| = 2\pi/\lambda$: No. waves per meter
  2. $\vec{k}/|\vec{k}|$: the wave's direction of prop.
- If signal have only a narrow band of spectral components, (i.e. all $\approx w$), we can replace $|k|$ with $w_0/c = 2\pi/\lambda_0$.
  - Example: Linear array along x-axis:

$$W(-k\sin\phi) = \frac{\sin\frac{k_x D\sin\phi}{2}}{\frac{k_x \sin\phi}{2}}$$

$$\Updownarrow$$

$$W(-2\pi\sin\phi/\lambda_0) = W''(\phi) = \lambda_0\frac{\sin D'\pi\sin\phi}{\pi\sin\phi}, \quad D' = D/\lambda_0$$

- $W''(\phi) = W''(\phi + \pi)$, i.e. periodic!! $W(k)$ is not!
- Often $W(u, v)$, $u = \sin\phi\,\cos\theta$, $v = \sin\phi\,\sin\theta$

Co-array for continuous apertures

- $c(\vec{\chi}) \equiv \int w(\vec{x})w(\vec{x}+\vec{\chi})d\vec{x}$, $\vec{\chi}$ called lag and its domain *lag space*.
- Important when array processing algorithms employ the wave's spatiotemporal correlation function to characterize the wave's energy.
- Fourier transform of $c(\vec{\chi})(=|W(\vec{k})|^2)$ gives a smoothed estimate of the power spectrum $S_f(\vec{k}, w)$.

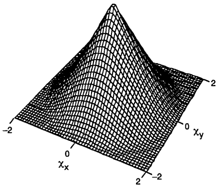

Figure 3.10 The cross-section of the co-array of a circular aperture of radius $R = 1$ is plotted as a function of radial distance χ in lag space.

Outline

Periodic spatial sampling in one dimension

- Array:
  - Consists of individual sensors that sample the environment spatially
  - Each sensor could be an aperture or omni-directional transducer
  - Spatial sampling introduces some complications (Nyquist sampling, folding, ...)
- Question to be asked/answered:
  When can $f(x, t_0)$ be reconstructed by $\{y_m(t_o)\}$?
  - $f(x, t)$ is the continuous signal and
  - $\{y_m(t)\}$ is a sequence of temporal signals where $y_m(t) = f(md, t)$, d being the spatial sampling interval.

Periodic spatial sampling in one dimension ...

- Sampling theorem (Nyquist):
  If a continuous-variable signal is band-limited to frequencies below k_0, then it can be periodically sampled without loss of information so long as the sampling period $d \leq \pi / k_0 = \lambda_0 / 2$.

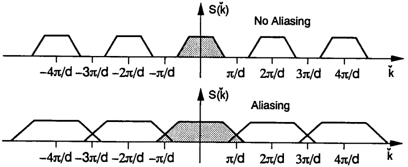

Figure 3.13 The periodic spectrum $S(\check{k})$ is equal to the sum of periodic replications of the spectrum $S_c(k)$. In this case the periodic replications do not overlap because $S_c(k)$ is bandlimited to a frequency $k_0 \leq \pi/d$. When the spectrum $S_c(k)$ is not bandlimited to frequencies below π/d, one period of the periodic spectrum $S(\check{k})$ does not equal $S_c(k)$. This phenomenon is called *aliasing*.

Periodic spatial sampling in one dimension ...

- Periodic sampling of one-dimensional signals can be straightforwardly extended to multidimensional signals.
- “Rectangular / regular” sampling not necessary for multidimensional signals.

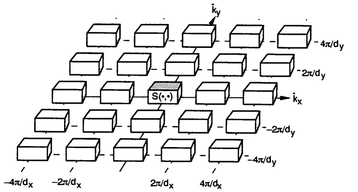

Figure 3.14 $S(\check{k}_x, \check{k}_y)$ can be interpreted as the periodic extension of $S_c(k_x, k_y)$. When $s_c(x, y)$ is bandlimited and the sampling intervals d_x and d_y are chosen small enough (as shown here), $s_c(x, y)$ may be reconstructed from the samples $s(m, n)$.

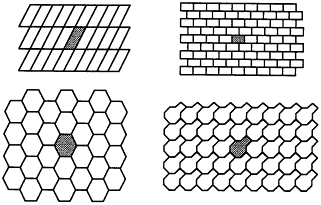

Figure 3.16 Several differently shaped baseband regions $\mathfrak{R}$, when periodically extended in a manner consistent with Cartesian sampling, completely cover the two-dimensional frequency plane.

Outline

Finite Continuous Apetrures

- Apertures and Arrays
- Aperture function
- Classical resolution
- Geometrical optics
- Ambiguities & Aberrations

Spatial sampling

- Sampling in one dimension

Arrays of discrete sensors

- Regular arrays
- Grating lobes
- Element response
- Irregular arrays

Regular arrays

- Assume point sources ($W_{tot} = W_{array} \cdot W_{el}$)).
- Easy to analyze and fast algorithms available (FFT).

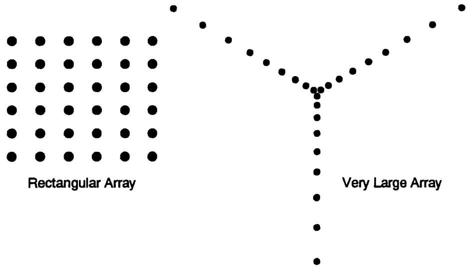

Figure 3.17 Two arrays of discrete sensors are shown. On the left, rectangular array has periodically spaced sensors. The *VLA* shown on the right has power-law spaced sensors along each arm (see Prob. 3.16).

Regular arrays; linear array

- Consider linear array; M equally spaced ideal sensor with inter-element spacing d along the x direction.
  - The discrete aperture function, w_m.
  - The discrete aperture smoothing function, $W(k)$:

$$W(k) \equiv \sum_m w_m e^{\jmath kmd}$$

  - Spatial aliasing given by d relative to λ.

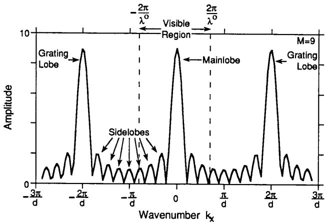

Figure 3.20 The aperture smoothing function magnitude $|W(k)|$ for uniform shading is plotted for a nine-sensor regular linear array. This spatial spectrum has period $k = 2\pi/d$. The visible region of the aperture smoothing function is that part for which $-2\pi/\lambda^o \leq k_x^o \leq 2\pi/\lambda^o$. What might be called secondary mainlobes—those not located at the origin—are termed grating lobes.

Grating lobes

- Given an linear array of M sensors with element spacing d.
  - $W(k) = \frac{\sin kMd/2}{\sin kd/2}$.
  - Mainlobe given by $D = Md$.
  - Gratinglobes (if any) given by d.
  - Maximal response for $\phi = 0$. Does it exist other ϕ_g with the same maximal response?
    $k_x = 2\frac{\pi}{\lambda}\sin\phi_g \pm 2\frac{\pi}{d}n \Rightarrow \sin\phi_g = \pm\frac{\lambda}{d}n$.
  - $n = 1$: No gratinglobes for $\lambda/d > 1$, i.e. $d < \lambda$.
  - $d = 4\lambda$:
    $\sin\phi_g \pm n \cdot 1/4 \Rightarrow \phi_g = \pm 14.5°, \pm 30°, \pm 48.6°, \pm 90°$.

Element response

- If the elements have finite size:

$$W_e(\vec{k}) = \int_{-\infty}^{\infty} w(\vec{k}) e^{\jmath \vec{k} \cdot \vec{x}} d\vec{x}$$

  - If linear array:
    Continuous aperture "devided into" M parts of size d
    Each single element: $\frac{sin(kd/2)}{k/2} \rightarrow$ first zero at $k = 2\pi/d$
- Total response:
  $W_{\text{total}}(\vec{k}) = W_e(\vec{k}) \cdot W_a(\vec{k})$,
  where $W_a(\vec{k})$ is the array response when point sources are assumed.

Irregular arrays

- Discrete co-array function:
  - $c(\vec{\chi}) = \sum_{(m_1,m_2)\in\vartheta(\vec{\chi})} w_{m_1} w^*_{m_2}$, where $\vartheta(\vec{\chi})$ denotes the set of indices (m_1, m_2) for which $\vec{x}_{m_2} - \vec{x}_{m_1} = \vec{\chi}$.
  - $0 \leq c(\vec{\chi}) \leq M = c(\vec{0})$.
  - Equals the inverse Fourier Transform of $|W(\vec{k})|^2$
    $\Rightarrow$ sample spacing in the lag-domain must be small enough to avoid aliasing in the spatial power spectrum.
  - Redundant lag: The number of distinct baselines of a given length is grater than one.

Examples

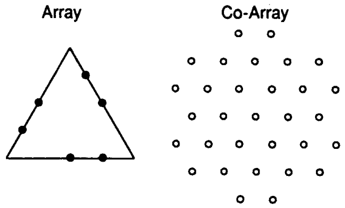

Figure 3.22 The Haubrich array shown on the left has the co-array on the right. Because there are no redundant baselines in the array, the co-array values are all equal to one except at the origin (zero lag), where the co-array value is M.

Examples ...

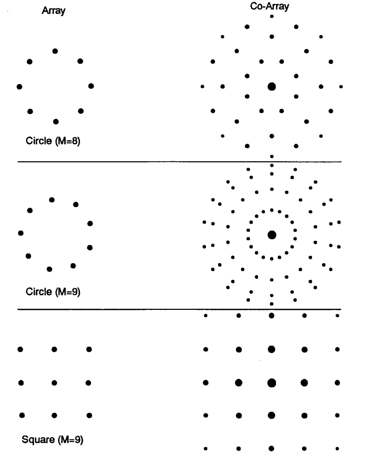

Figure 3.23 The sensor locations for two circular arrays and a square array are shown in the left column. The first of the circular arrays contains eight sensors; the square array and the remaining circular array each contain nine sensors. Their corresponding co-arrays are shown in the right column. The area of the circles denoting co-array locations is proportional to the redundancy at that lag. The redundancy at the origin of a co-array always equals *M*. Note how these regular array geometries lead to co-arrays spanning complicated spatial regions.

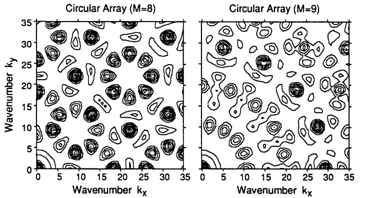

Figure 3.25 The panels depict the Fourier Transforms of the co-arrays for the circular arrays depicted in Fig. 3.23. The computations for the eight-sensor array are shown on the left, the nine-sensor on the right. The spectra are plotted only over the first quadrant of wavenumber space. Peak height can be judged by the number of contours encircling the peak.

Irregular arrays

- Sparse arrays
  - Underlying regular grid, all position not filled.
  - Position fills to acquire a given co-array
    - Non-redundant arrays with minimum number of gaps
    - Maximal length redundant arrays with no gaps.
  - Sparse array optimization
    - Irregular arrays can give regular co-arrays ...

Examples

- Non-redundant arrays == Minimum hole arrays == Golumb arrays *1101*, *1100101*, *110010000101*
- Redundant arrays == Minimum redundancy arrays *1101*, *1100101*, *1100100101*

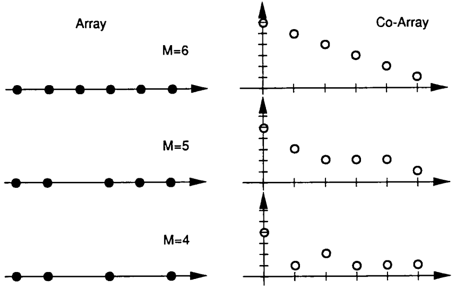

Figure 3.27 A six-sensor, filled array and its co-array are shown. Two arrays having the same aperture are derived by successively removing sensors from the array. This thinning procedure results in the depicted co-arrays. To derive the four-sensor perfect array, one must start with a seven-sensor filled array.

Random arrays

- $W(\vec{k}) = \sum_{m=0}^{M-1} e^{\jmath \vec{k}\cdot\vec{x}_m}$ (assumes unity weights)
- $E[W(\vec{k})] = \sum_{m=0}^{M-1} E[e^{\jmath \vec{k}\cdot\vec{x}_m}] = M \int p_x(\vec{x}_m) e^{\jmath \vec{k}\cdot\vec{x}_m} d\vec{x} = M \cdot \Phi_x(\vec{k})$
  i.e. Equals the array pattern of a continuous aperture where the probability density function plays the same role as the weighting function.
- $var[W(\vec{k})] = E[|W(\vec{k})|^2] - (E[W(\vec{k})])^2$
  - $E[|W(\vec{k})|^2] = E[\sum_{m_1=0}^{M-1} e^{\jmath \vec{k}\cdot\vec{x}_{m_1}} \cdot \sum_{m_2=0}^{M-1} e^{-\jmath \vec{k}\cdot\vec{x}_{m_2}}]$
    $= E[M \cdot 1 + \sum_{m_1, m_1 \neq m_2} e^{\jmath \vec{k}\cdot\vec{x}_{m_1}} \cdot \sum_{m_2} e^{-\jmath \vec{k}\cdot\vec{x}_{m_2}}]$
    Assumes uncorrelated x_m ($E[x \cdot y] = E[x] \cdot E[y]$)
    $\Rightarrow E[|W(\vec{k})|^2] = M + (M^2 - M)|\Phi_x(\vec{k})|^2$

  $\Rightarrow var[W(\vec{k})] = M - M|\Phi_x(\vec{k})|^2$